PAPER

2-Dimensional OVSF Spread/Chip-Interleaved CDMA

Le LIU[†a)], ***Student Member and*** **Fumiyuki ADACHI**[†], ***Member***

SUMMARY Multiple-access interference (MAI) limits the bit error rate (BER) performance of CDMA uplink transmission. In this paper, we propose a generalized chip-interleaved CDMA with 2-dimensional (2D) spreading using orthogonal variable spreading factor (OVSF) codes to minimize the MAI effects and achieve the maximum available time- and frequency-domain diversity gains. We present the code assignment for 2D spreading to provide users with flexible multi-rate data transmission. A computer simulation shows that by the joint use of 2D OVSF spreading and chip-interleaving, MAI-free transmission is possible for the quasi-synchronous DS- or MC-CDMA uplink, and hence the single-user frequency-domain equalization based on the MMSE criterion can be applied for signal detection. The BER performance in a time- and frequency-selective fading multiuser channel is theoretically analyzed and evaluated by both numerical computation and computer simulation.

key words: *CDMA, multi-rate, uplink transmission, chip interleaving, 2-dimensional OVSF spreading*

1. Introduction

In next generation mobile communications, a flexible support of low-to-high bit rate (or multi-rate) multimedia services is required [1], [2]. Using code division multiple access (CDMA) technique [3], multi-rate data transmission can be achieved by changing the number of parallel orthogonal spreading codes in the multicode transmission or by simply changing the spreading factor in the single-code transmission [4]–[6]. The well-known CDMA techniques include single-carrier direct sequence (DS)-CDMA [2], [4] using time-domain spreading and multicarrier (MC)-CDMA [7]–[10] using frequency-domain spreading. Recently, it was shown [2], [6] that the frequency-domain equalization (FDE) based on the minimum mean square error (MMSE) criterion can significantly improve the BER performance of DS-CDMA downlink transmission in a severe frequency-selective fading channel, compared to conventional coherent rake combining. The downlink DS-CDMA with MMSE-FDE can achieve almost the same BER performance as the downlink MC-CDMA.

However, in uplink transmission, different users' signals go through different channels and are asynchronously received, which produces multiple-access interference (MAI) and limits the uplink capacity. The suppression of MAI to increase the link capacity as well as to provide multi-rate services is a challenging task for the realization of the next generation mobile communication systems [11]. Although multiuser detection (MUD) [12], [13] can be used to mitigate the detrimental effects of MAI, the MUD algorithms are relatively complex, and their computational complexity increases exponentially with the number of users. MUD receivers at the base station also require the knowledge of all users' channels. In practice, however, the users' channel information needs to be estimated from the received signals and are prone to the MAI and noise. It has been shown by [14] that MUD is sensitive to time delay mismatch, especially in a near-far environment.

Chip repetition in the time-domain was proposed for asynchronous DS-CDMA uplink using coherent rake combing at the base station [15], where the user-specific frequency shift is used to separate simultaneously accessing users. Recently, chip-interleaving together with orthogonal spreading codes has been proposed for DS-CDMA to cancel the MAI in a quasi-synchronous multipath channel [16], [17]. In [16] and [17], it was found that chip-interleaved DS-CDMA with cyclic prefix as a guard interval (GI) can provide better performance by using simple FDE. Provided that the propagation channel delays and transmit timings of different users are within the GI, MAI-free transmission is guaranteed by user-specific orthogonal codes. More recently, we have introduced 2-dimensional (2D) spreading using orthogonal variable spreading factor (OVSF) codes [18], [19] for the chip-interleaved DS-CDMA uplink transmission [20], [21]. A joint use of 2D OVSF spreading and chip-interleaving makes it possible to realize multi-rate transmission while avoiding high-complexity MUD processing.

In this paper, we extend this concept to a generalized chip-interleaved multi-rate (DS- and MC-) CDMA with 2D OVSF spreading for quasi-synchronous uplink transmission. This generalized scheme can provide either DS- or MC-CDMA with flexible muti-rate/multi-connection services in both downlink and quasi-synchronous uplink. In this paper, we consider multi-rate, single-code CDMA uplink transmission in a multiuser environment and present the optimum code assignment for 2D OVSF spreading with the given overall spreading factor, $SF = SF_t \times SF_f$, where SF_f is the spreading factor of the 1st OVSF spreading code for multi-rate services per user and SF_t is the spreading factor of the 2nd one for orthogonal multiuser multiplexing. Through appropriate code assignment of 2D OVSF spreading, not only the maximum time- and frequency-domain diversity gains can be achieved but also a flexible support for

Manuscript received October 20, 2005.
Manuscript revised June 14, 2006.

[†]The authors are with the Dept. of Electrical and Communication Engineering,Tohoku University, Sendai-shi, 980-8579 Japan.
a) E-mail: liule@mobile.ecei.tohoku.ac.jp

DOI: 10.1093/ietcom/e89–b.12.3363

the low-to-high bit rate of multimedia services is possible. Most of the previous works aiming at MAI suppression focused on the uncoded case. However, analyses of different schemes without coding do not always properly predict the performances of those with coding [22], [23]. In this paper, the turbo-coded BER performance of our proposed 2D OVSF spread/chip-interleaved CDMA is evaluated and compared with that of conventional multiuser CDMA with MUD reception.

The remainder of this paper is organized as follows. Section 2 presents the uplink transmission model of 2D OVSF spread/chip-interleaved DS- and MC-CDMA. Then, the code assignment for the 2D OVSF spreading is discussed in Sect. 3. In Sect. 4, an exact theoretical analysis of the conditional BER performance is presented taking the fading Doppler spread into account. Using the derived conditional BER expression, the average BER is evaluated by the Monte-Carlo numerical computation method in Sect. 5, which is confirmed by computer simulation. The turbo-coded BER performance obtained by computer simulation is also presented in Sect. 5 and the impact of the fading Doppler frequency on the BER performance is discussed. Finally, Sect. 6 offers concluding remarks and future work.

2. Transmission System Model

We assume the multi-rate, single-code CDMA uplink transmission with U active users (this scheme can also be applied to the CDMA downlink transmission). The transmission model is illustrated in Fig. 1, where only the uth user, $u = 0 \sim U-1$, is considered (this scheme can also be applied to downlink transmission). Here, we assume the square-root Nyquist chip shaping filter at the transmitter and the same filter at the receiver as the chip-matched filter. Ideal chip sampling timing is assumed at the receiver. Therefore, the chip-spaced discrete-time signal representation is used throughout the paper. In this paper, $|a|$ denotes the amplitude of complex-valued a, $\lfloor a \rfloor$ is the largest integer smaller than or equal to the real-valued variable a and $\lceil a \rceil$ is the smallest integer larger than or equal to a. $E[\cdot]$ denotes the ensemble average operation and x mod y is the modulus operation to get the remainder after division x/y.

2.1 Transmitted Signal

We consider the block data transmission of N_c/SF_f^u symbols, where SF_f^u is the spreading factor of the uth user's 1st OVSF spreading code $\{c_u^{SF_f^u}(t);\ t = 0 \sim SF_f^u - 1\}$ with $|c_u^{SF_f^u}(t)| = 1$ and N_c is the FFT/IFFT block size for FDE used at the base-station receiver. The uth user's data symbol sequence $\{d_u(n);\ n = 0 \sim (N_c/SF_f^u - 1)\}$ with $E[|d_u(n)|^2] = 1$ is spread by $\{c_u^{SF_f^u}(t);\ t = 0 \sim SF_f^u - 1\}$ and is further multiplied by a binary scramble sequence $\{c_u^{scr}(t);\ t = 0 \sim N_c - 1\}$ to produce the DS-CDMA signal $s_u^{DS}(t)$. $s_u^{DS}(t)$ can be expressed as

$$s_u^{DS}(t) = c_u^{scr}(t) d_u\left(\left\lfloor t/SF_f^u \right\rfloor\right) c_u^{SF_f^u}(t \bmod SF_f^u). \tag{1}$$

If N_c-point IFFT is applied to $s_u^{DS}(t)$, an MC-CDMA

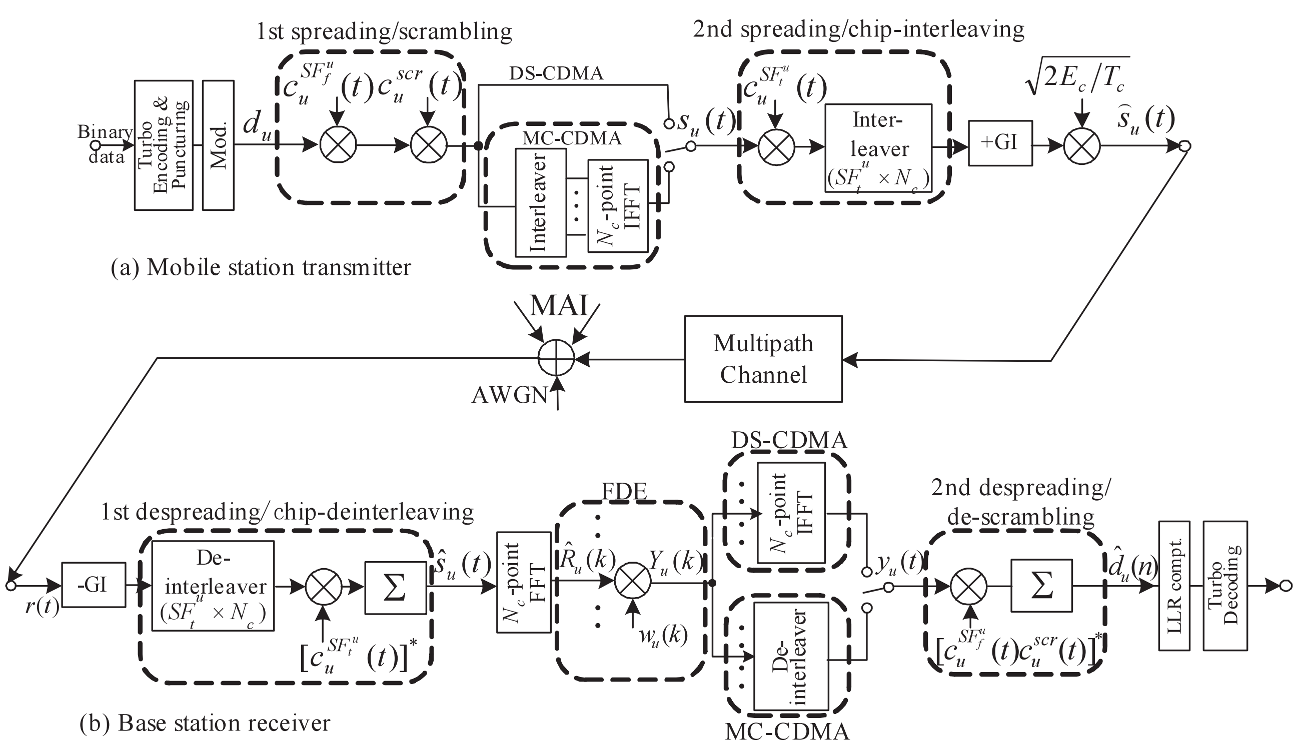

Fig. 1 Uplink transmitter/receiver structure.

signal $s_u^{MC}(t)$ is generated. In order to make better use of the channel frequency-selectivity, $SF_f^u \times (N_c/SF_f^u)$-chip interleaving is performed before IFFT. Then, the data chips are distributed, with an equal distance of (N_c/SF_f^u) subcarriers, over N_c subcarriers. $s_u^{MC}(t)$ can be expressed as

$$s_u^{MC}(t) = \frac{1}{\sqrt{N_c}} \sum_{n=0}^{N_c/SF_f^u-1} \sum_{i=0}^{SF_f^u-1} \left[s_u^{DS}(nSF_f^u + i) \times \exp\left\{ j2\pi \frac{t}{N_c} \cdot \left(n + i\frac{N_c}{SF_f^u} \right) \right\} \right]. \tag{2}$$

Next, the N_c-chip CDMA signal $s_u(t)$ is spread by the 2nd OVSF spreading code $\{c_u^{SF_t^u}(t);\ t = 0 \sim SF_t^u - 1\}$ with spreading factor SF_t^u. Then, the chip-interleaving, as shown in Fig. 2, is performed with column-wise input and row-wise output. As illustrated in Fig. 3, the 2D OVSF spreading for DS-CDMA is done in the time-domain only; while, in the case of MC-CDMA, data is spread in both the time- and frequency-domain. The interleaver output chip sequence is divided into N_c-chip blocks. Before transmission, an N_g-chip GI is inserted every N_c-chip block to avoid inter-block interference (IBI). The transmitted signal can be expressed using equivalent lowpass representation as

$$\widehat{s}_u(t) = \sqrt{2E_c/T_c}\, s_u(t \bmod N_c) c_u^{SF_t^u}(\lfloor t/N_c \rfloor) \tag{3}$$

for $t = -N_g \sim SF_t^u(N_c+N_g)-N_g-1$, where E_c is the average chip energy and T_c is the chip duration.

2.2 Channel

The GI-inserted signal is transmitted over a frequency- and time-selective fading channel. Assuming that the channel has L independent propagation paths, the discrete-time impulse response $h_u(\tau, t)$ of the uth user at time t is expressed as [24]

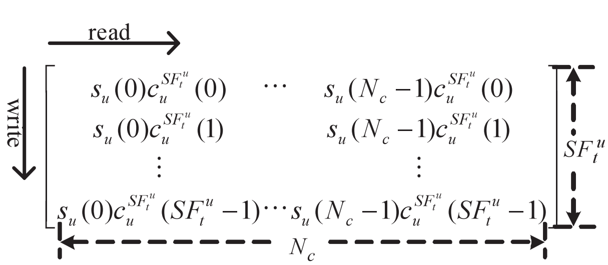

Fig. 2 Chip-interleaving.

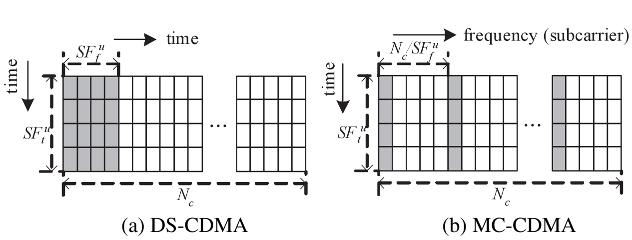

Fig. 3 2D OVSF spreading and chip-interleaving

$$h_u(\tau, t) = \sum_{l=0}^{L-1} h_{u,l}(\lfloor t/T \rfloor)\delta(\tau - \tau_{u,l}), \tag{4}$$

where $h_{u,l}(\lfloor t/T \rfloor)$ and $\tau_{u,l}$ are respectively the complex-valued path gain and time delay of the lth path with $\sum_{l=0}^{L-1} E[|h_{u,l}(t)|^2] = 1$, and $\delta(x)$ is the delta function. We assume a block fading, where the path gains $h_{u,l}(\lfloor t/T \rfloor)$ remain constant over one block interval $T = T_c(N_c + N_g)$, but vary block-by-block. $\tau_{u,l}$ is assumed to be T_c-spaced time delays and equal to $\tau_{u,l} = \tau_u + lT_c$, $l = 0 \sim L-1$, where τ_u is the uth user's transmit timing offset. The maximum time delay of $\{\tau_{u,l}\}$ is assumed to be shorter than the GI (we assume some transmit timing control).

2.3 Received Signal

The sum of U users' faded signals is received by a base-station receiver. The received signal is sampled at the chip rate and the GI is removed first. The GI-removed received signal can be written as

$$r(t) = \sum_{u=0}^{U-1} \sum_{l=0}^{L-1} h_{u,l}(\lfloor t/T \rfloor)\widehat{s}_u(t - \tau_{u,l}) + n(t), \tag{5}$$

where $n(t)$ is the zero-mean additive white Gaussian noise (AWGN) with the variance of $2N_0/T_c$ (N_0 is the one-sided power spectrum density).

2.4 Chip-Deinterleaving/1st Despreading

Chip-deinterleaving is illustrated in Fig. 4. As shown in Fig. 4, $r(t)$ is $SF_t^u \times N_c$-chip deinterleaved and then the 1st despreading is performed using the 2nd OVSF spreading code $\{c_u^{SF_t^u}(t);\ t = 0 \sim SF_t^u - 1\}$ as

$$\hat{s}_u(t) = \frac{1}{SF_t^u} \sum_{i=0}^{SF_t^u-1} r(t + iN_c)\left[c_u^{SF_t^u}(i)\right]^* \tag{6}$$

for $t = 0 \sim N_c - 1$, where $(\cdot)^*$ denotes the conjugate operation. Since $\{c_u^{SF_t^u}(t);\ u = 0 \sim U-1\}$ are orthogonal, the MAI can be cancelled if the fading is very slow so that the path gains stay almost constant over at least SF_t^u consecutive blocks.

2.5 MMSE-FDE

After despreading, N_c-point FFT is applied to decompose

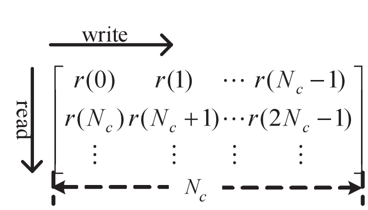

Fig. 4 Chip-deinterleaving.

the despread signal $\{\hat{s}_u(t); t = 0 \sim (N_c-1)\}$ into N_c frequency components $\{\hat{R}_u(k); k = 0 \sim (N_c-1)\}$ as

$$\hat{R}_u(k) = \frac{1}{\sqrt{N_c}} \sum_{t=0}^{N_c-1} \hat{s}_u(t) \exp\left(-j2\pi k \frac{t}{N_c}\right). \quad (7)$$

If $\sum_{u=0}^{U-1}(SF_t^u)^{-1} \leq 1$ and U users are assigned different 2nd OVSF spreading codes, the MAI can be perfectly eliminated and hence, single-user one-tap MMSE-FDE can be carried out on each frequency component as

$$Y_u(k) = w_u(k)\hat{R}_u(k), \quad (8)$$

where $w_u(k)$ is the MMSE-FDE weight given by [2], [6]

$$w_u(k) = \frac{H_u^*(k)}{|H_u(k)|^2 + (SF_t^u \cdot E_c/N_0)^{-1}} \quad (9)$$

with $H_u(k)$ being the kth frequency component of the uth user's channel gain.

On the other hand, if $\sum_{u=0}^{U-1}(SF_t^u)^{-1} > 1$, the same 2nd OVSF spreading code is assigned to more than one users. Users with the same OVSF spreading code belong to the same group and they are interference-free from other groups with different 2nd OVSF spreading codes. If there are more-than-one users in some groups, the MAI is produced in those groups and the MMSE-MUD is necessary to minimize the residual MAI. However, since the number of users in those groups is still much smaller than U, MMSE-MUD is much less complex than that considered in [12], which needs to combat the MAI from all U users.

For DS-CDMA, an N_c-point IFFT is applied to $\{Y_u(k); k = 0 \sim N_c - 1\}$ to get the time-domain chip sequence:

$$y_u^{DS}(t) = \frac{1}{\sqrt{N_c}} \sum_{k=0}^{N_c-1} Y_u(k) \exp\left(j2\pi t \frac{k}{N_c}\right) \quad (10)$$

for $t = 0 \sim N_c - 1$. On the other hand, as shown in Fig. 1, the MC-CDMA signal $y_u^{MC}(t)$ is obtained directly from the frequency-domain deinterleaver as

$$y_u^{MC}(t) = Y_u\left((t \bmod SF_f^u) \cdot (N_c/SF_f^u) + \lfloor t/SF_f^u \rfloor\right) \quad (11)$$

for $t = 0 \sim N_c - 1$.

2.6 2nd Despreading

The 2nd despreading using the 1st OVSF spreading code $c_u^{SF_f^u}(t)$ is performed to get the decision variable $\hat{d}_u(n)$ associated with $d_u(n)$ as

$$\hat{d}_u(n) = \frac{1}{SF_f^u} \sum_{t=nSF_f^u}^{(n+1)SF_f^u-1} y_u(t) \left[c_u^{SF_f^u}(t) c_u^{scr}(t)\right]^*, \quad (12)$$

based on which the log-likelihood ratio (LLR) [22], [23] is computed for turbo decoding.

2.7 LLR Computation

A sequence of soft values for turbo decoding can be generated using LLR [22]. The LLR value should be computed taking into account the equivalent channel gain and residual MAI after FDE [25]. When the channel is time-selective due to the fading Doppler spread, even if all users are assigned different 2nd OVSF spreading codes, the MAI cannot be cancelled completely. According to the central limit theorem, the residual interference-plus-noise can be treated as a Gaussian process [13], [25]. We can show that Eq. (12) can be expressed as

$$\hat{d}_u(n) = \mu_u(n)d_u(n) + \xi_{SI}(n) + \xi_{MAI}(n) + \xi_{noise}(n), \quad (13)$$

where $\mu_u(n)$ is the equivalent channel gain for the uth user's signal and $\xi_{SI}(n)$, $\xi_{MAI}(n)$ and $\xi_{noise}(n)$ respectively represent the self interference (SI), MAI and noise components. $\hat{d}_u(n)$ is a random variable with mean $\mu_u(n)d_u(n)$ and variance $2\sigma_u^2(n)$ ($\mu_u(n)$ and $2\sigma_u^2(n)$ are derived in Sect. 4). Assuming quaternary phase shift keying (QPSK) data-modulation, the LLRs for the 1st bit and 2nd bit of the nth QPSK symbol are given by [12], [13]

$$LLR = \begin{cases} \mathrm{Re}\left\{\mu_u^*(n) \cdot \hat{d}_u(n)\right\}/2\sigma_u^2(n) & \text{for the 1st bit} \\ \mathrm{Im}\left\{\mu_u^*(n) \cdot \hat{d}_u(n)\right\}/2\sigma_u^2(n) & \text{for the 2nd bit} \end{cases}. \quad (14)$$

3. Code Assignment for 2D OVSF Spreading

The overall spreading factor of the uth user's 2D OVSF codes is $SF^u = SF_t^u \times SF_f^u$. The total data rate normalized by the chip (or sample) rate for the multi-rate and multiuser case is defined as [5]

$$R_{total} = \sum_{u=0}^{U-1}(SF_t^u \times SF_f^u)^{-1} < 1. \quad (15)$$

The 1st OVSF spreading code of spreading factor SF_f^u is for multi-rate services per user and SF_f^u can be arbitrarily set according to the requested data rate, independently of the FFT block size N_c, but $SF_f^u \leq N_c$. The 2nd OVSF spreading code is for orthogonal multiuser multiplexing. The MAI is cancelled due to the orthogonality property of the 2nd OVSF spreading codes. However, the code orthogonality may be distorted in a time-selective fading channel. If the path gain stays almost constant over SF_t^u consecutive blocks, the MAI resulting from the orthogonality distortion may not be severe. Hence, SF_t^u should be smaller than the maximum permitted value SF_t, which is determined by the fading Doppler frequency.

For the assignment of 2D OVSF spreading factor (SF_t^u, SF_f^u), SF_t^u is determined by the number of users and then SF_f^u is set at SF^u/SF_t^u, where the total spreading factor SF^u is inverse-proportionate to the data rate. Therefore, the assignment of (SF_t^u, SF_f^u) is independent of the channel frequency-selectivity. As discussed in [26], the frequency-selectivity or the delay spread only affects the performance of 2D OVSF spread CDMA. In general, as the delay spread decreases, the frequency-selectivity becomes weaker, resulting in less frequency-diversity effect. In 2D OVSF spread DS-CDMA, the data symbol is always spread over the entire signal bandwidth, yielding the same frequency diversity gain irrespective of SF_f^u. On the other hand, in the case of 2D OVSF spread MC-CDMA, the data symbol is spread over only SF_f^u subcarriers. Therefore, the achievable frequency-diversity gain decreases as SF_f^u decreases.

3.1 Multi-Rate/Single-Connection Case

3.1.1 SF_t^u-Code Assignment

If $U < SF_t$ and $U = 2^k$ ($k = 0, 1, \cdots$), all users can be assigned $SF_t^u = 2^k$. An MAI-free channel is constructed after the chip-deinterleaving/1st despreading as described in Sect. 2.4. The MUD problem is converted into a set of equivalent single-user detection problems and the use of complicated MUD receivers can be avoided. If $U < SF_t$ but $2^{k-1} < U < 2^k$, $(2^k - U)$ users among U users can be assigned $SF_t^u = 2^{k-1}$ and then the other $(2U - 2^k)$ users can use $SF_t^u = 2^k$. By doing so, all U users are orthogonal if Eq. (15) holds.

If $U > SF_t$, users are partitioned into SF_t groups first. Each group uses a different OVSF spreading code with the spreading factor SF_t. Users with the same 2nd OVSF spreading code belong to the same group. Users in the same group are interference-free from other groups. We then apply MUD per group, which is practically feasible since the number of users per group is at most $\lceil U/SF_t \rceil$, much smaller than U. In contrast, the MUD for the conventional DS- or MC-CDMA needs to suppress the MAI from all $(U - 1)$ interfering users, and thus has prohibitive complexity.

3.1.2 SF_f^u-Code Assignment

After setting the value of SF_t^u for each user, SF_f^u can be set equal to SF^u/SF_t^u, where the overall spreading factor SF^u $(= SF_t^u \times SF_f^u)$ is determined by the uth user's data rate. Therefore, our proposed code assignment achieving MAI-free uplink transmission is very flexible for multi-rate services.

3.1.3 Example

One example for the spreading code assignment is shown in Fig. 5, which illustrates the OVSF code tree [18]. We assume the maximum permitted spreading factor is $SF_t = 16$. There are $U = 5$ active users and among them, 2 users with rate R_L, 2 users with rate $2R_L$ and 1 user with rate $4R_L$, where the lowest data rate R_L corresponds to $(SF_t^u \times SF_f^u)^{-1} = 1/16$. According to Sect. 3.1.1, two users may be assigned $SF_t^u = 8$ and the other three users $SF_t^u = 4$. We assume user $u = 0$ with $R_L = (8 \times 2)^{-1}$, user $u = 1$ with $R_L = (4 \times 4)^{-1}$, user $u = 2$ with $2R_L = (8 \times 1)^{-1}$, user $u = 3$ with $2R_L = (4 \times 2)^{-1}$, and user $u = 4$ with $4R_L = (4 \times 1)^{-1}$. Then, OVSF codes $c_{8,1}$ and $c_{8,2}$, are selected as the spreading codes, $c_{u=0}^{SF_t^0}(t)$ and $c_{u=2}^{SF_t^2}(t)$ with $SF_t^0 = SF_t^2 = 8$, to maintain the orthogonality between each other. As shown in Fig. 5, they have the same mother code $c_{4,1}$ and therefore, OVSF codes $c_{4,2}$, $c_{4,3}$, and $c_{4,4}$ should be assigned to users $u = 1, 3, 4$, respectively.

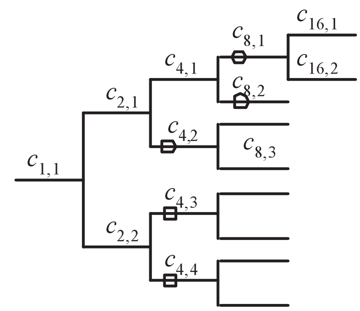

Fig. 5 OVSF code tree.

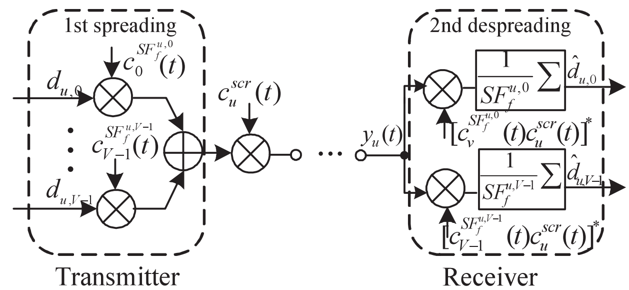

Fig. 6 Muti-rate/multi-connection for the uth user.

3.2 Multi-Rate/Multi-Connection Case

Until now, we have discussed multi-rate, single-connection transmission. Our proposed scheme can be extended allow multiple connections per user. Data sequences of multiple connections are channel-coded, data-modulated and spread using different 1st OVSF spreading codes. Multiple connections are independent each other and depend on their own requested communication qualities and types of data traffic (i.e., continuous traffic or packet traffic) [5].

As shown in Fig. 6, there are V parallel connections for the uth user. The vth data-modulated symbol sequence $\{d_{u,v}(n)\}$ of the uth user is spread using the 1st OVSF spreading code $\{c_u^{SF_f^{u,v}}(t);\ t = 0 \sim SF_f^{u,v} - 1\}$ with spreading factor $SF_f^{u,v}$. The resultant V parallel chip sequences are summed up and further multiplied by a binary scramble sequence $\{c_u^{scr}(t);\ t = 0 \sim N_c - 1\}$ to produce the N_c-chip DS-CDMA signal, which can be expressed as

$$s_u^{DS}(t) = c_u^{scr}(t) \sum_{v=0}^{V-1} d_{u,v}\left(\left\lfloor t/SF_f^{u,v} \right\rfloor\right) c_u^{SF_f^{u,v}}(t \bmod SF_f^{u,v}). \tag{16}$$

In the case of single connection ($V = 1$), Eq. (16) reduces to

Eq. (1). For the sake of convenience, the equivalent spreading factor $SF^u_{f,eq}$ is defined as

$$SF^u_{f,eq} = 1 \Big/ \sum_{v=0}^{V-1} (SF_f^{u,v})^{-1} \leq 1. \tag{17}$$

The same 2nd spreading with the spreading factor SF^u_t is applied to $s^{DS}_u(t)$ as in the single-connection case. Therefore, the normalized total data rate for multi-rate/multi-connection/multiuser transmission becomes

$$R_{total} = \sum_{u=0}^{U-1} \left[\left(SF^u_t \cdot SF^u_{f,eq} \right)^{-1} \right] \leq 1. \tag{18}$$

At the receiver side shown in Fig. 6, the 2nd despreading using the 1st OVSF spreading code $c_u^{SF_f}(t)$ is performed to get the decision variable $\hat{d}_{u,v}(n)$ for the detection of $d_{u,v}(n)$ as

$$\hat{d}_{u,v}(n) = \frac{1}{SF_f^{u,v}} \sum_{t=nSF_f^{u,v}}^{(n+1)SF_f^{u,v}-1} y_u(t) \left\{ c_u^{SF_f^{u,v}}(t) c_u^{scr}(t) \right\}^*, \tag{19}$$

based on which data symbol demodulation and turbo decoding are carried out for the vth connection. $y_u(t)$ in Eq. (19) is given by Eq. (10).

For MC-CDMA, we apply $SF^u_{f,eq} \times (N_c/SF^u_{f,eq})$-chip interleaving to $s^{DS}_u(t)$ and then, an N_c-point IFFT is used to get

$$s_u^{MC}(t) = \frac{1}{\sqrt{N_c}} \sum_{n=0}^{(N_c/SF^u_{f,eq}-1)} \sum_{m=0}^{(SF^u_{f,qu}-1)} \left[c_u^{scr}\left(nSF^u_{f,eq} + m \right) \times \sum_{v=0}^{V-1} d_{u,v}(n) c_u^{SF_f^{u,v}}(m) \exp\left\{ \frac{j2\pi t}{N_c} \left(n + m \frac{N_c}{SF^u_{f,eq}} \right) \right\} \right]. \tag{20}$$

The same 2nd spreading is also used as in the single-connection case. The decision variable $\hat{d}_{u,v}(n)$ is obtained using Eq. (19), where $y_u(t)$ is given by Eq. (11) for MC-CDMA.

3.3 Special Cases

If we set $V = 1$ and $SF^u_f = 1$, our proposed 2D OVSF spread DS-CDMA becomes chip-interleaved block spread DS-CDMA [16], [17] and our 2D OVSF spread MC-CDMA becomes MC/DS-CDMA [8], where different narrowband DS-CDMA signal is transmitted on each subcarrier.

In this paper, OVSF spreading codes are used to separate users in the time-domain. If we use the orthogonal phase-rotating sequences (or the frequency-shifting sequences), given by

$$c_u^{SF^u_t}(t) = \exp\left\{ -j2\pi u \frac{t}{SF^u_t} \right\} \quad \text{for } u = 0 \sim SF^u_t - 1, \tag{21}$$

instead of OVSF spreading codes, 2D OVSF DS-CDMA becomes the variable spreading and chip repetition factor (VSCRF) based CDMA [15]. The use of the orthogonal phase-rotating sequences results in non-overlappping comb-shaped frequency spectra of different users and hence no MAI is produced.

4. BER Analysis

For theoretical analysis, we assume V parallel connections for each user and each connection uses the same $SF_f^{u,v} = SF^u_f$ but every user has a different (SF^u_t, SF^u_f) pair. N_c-chip CDMA signal $s_u(t)$, given by Eq. (16) for DS-CDMA and Eq. (20) for MC-CDMA, is transmitted after the insertion of GI over a frequency-selective fading channel. Different user's fading channels are independent each other. Without loss of generality, we assume the ideal slow transmit power control for all users.

4.1 Decision Variable and Equivalent Channel Gain

Substituting Eqs. (3)–(6) into Eq. (7) gives

$$\hat{R}_u(k) = \sqrt{2E_c/T_c} S_u(k) H_u(k) + \sqrt{2E_c/T_c} \sum_{\substack{u'=0 \\ \neq u}}^{U-1} S_{u'}(k) Z_{u'}(k) + \Pi(k) \tag{22}$$

for $k = 0 \sim N_c - 1$, where u' denotes the interfering user and the 1st, 2nd and 3rd terms represent the desired signal, MAI and AWGN components, respectively, with

$$\begin{cases} S_u(k) = \dfrac{1}{\sqrt{N_c}} \displaystyle\sum_{t=0}^{N_c-1} s_u(t) \exp\left(-j2\pi k \frac{t}{N_c} \right) \\ H_u(k) = \dfrac{1}{SF_t} \displaystyle\sum_{i=0}^{SF^u_t-1} \sum_{l=0}^{L-1} h_{u,l}(i) \exp\left(-j2\pi k \frac{\tau_{u,l}}{N_c} \right) \\ Z_{u'}(k) = \dfrac{1}{SF_t} \displaystyle\sum_{i=0}^{SF^u_t-1} \left[\begin{array}{l} c_{u'}^{SF^{u'}_t}(i) \left\{ c_u^{SF^u_t}(i) \right\}^* \\ \times \displaystyle\sum_{l=0}^{L-1} h_{u',l}(i) \exp\left(-j2\pi k \frac{\tau_{u',l}}{N_c} \right) \end{array} \right] \\ \Pi(k) = \dfrac{1}{\sqrt{N_c}} \displaystyle\sum_{t=0}^{N_c-1} \eta(t) \exp\left(-j2\pi k \frac{t}{N_c} \right) \end{cases}. \tag{23}$$

As shown in Eqs. (8) and (9), MMSE-FDE is applied to $\hat{R}_u(k)$ to obtain $Y_u(k)$, followed by IFFT to get the time-domain signal $y_u(t)$ given as Eq. (10). The decision variable $\hat{d}_{u,v}(n)$ is obtained by substituting Eq. (10) into Eq. (19).

For DS-CDMA, we substitute Eq. (16) into Eq. (23) and then use Eqs. (22), (8), and (10) to obtain the vth connection of the uth user $\hat{d}_{u,v}(n)$. On the other hand, for MC-CDMA, we substitute Eq. (20) into Eq. (23) and then using Eqs. (22), (8), and (11) to get $\hat{d}_{u,v}(n)$. $\hat{d}_{u,v}(n)$ can be expressed as

$$\hat{d}_{u,v}(n) = \mu_{u,v}(n) d_{u,v}(n) + \xi_{SI}(n) + \xi_{MAI}(n) + \xi_{noise}(n), \tag{24}$$

where $\mu_{u,v}(n)$, $\xi_{SI}(n)$, $\xi_{MAI}(n)$, and $\xi_{noise}(n)$ are respectively the equivalent channel gain, self-interference, MAI, and noise components, which are given by

$$\mu_{u,v}(n) = \begin{cases} \dfrac{1}{N_c}\sqrt{\dfrac{2E_c}{T_c}}\displaystyle\sum_{k=0}^{N_c-1} w_u(k)H_u(k) \quad \text{for DS-CDMA} \\ \dfrac{1}{SF_f^u}\sqrt{\dfrac{2E_c}{T_c}}\displaystyle\sum_{i=0}^{SF_f^u-1} w_u\left(n+i\cdot\dfrac{N_c}{SF_f^u}\right)H_u\left(n+i\cdot\dfrac{N_c}{SF_f^u}\right) \\ \qquad\qquad \text{for MC-CDMA} \end{cases} \tag{25}$$

$$\xi_{SI}(n) = \begin{cases} \dfrac{1}{SF_f^u}\displaystyle\sum_{t=nSF_f^u}^{(n+1)SF_f^u-1}\left\{c_u^{SF_f^u}(t)c_u^{scr}(t)\right\}^* \dfrac{1}{N_c}\sum_{k=0}^{N_c-1} w_u(k)H_u(k) \\ \qquad \times\left[\sqrt{\dfrac{2E_c}{T_c}}\displaystyle\sum_{\substack{\tau=0\\ \neq t}}^{N_c-1} s_u^{DS}(\tau)\exp\left(j2\pi k\dfrac{t-\tau}{N_c}\right)\right] \\ \qquad\qquad \text{for DS-CDMA} \\ \dfrac{1}{SF_f^u}\displaystyle\sum_{\substack{v'=0\\ v'\neq v}}^{V-1}\sum_{i=0}^{SF_f^u-1}\left\{c_u^{SF_f^u}(i)\right\}^* c_{u,v'}^{SF_f^u}(i)d_{u,v'}(n) \\ \qquad \times\sqrt{\dfrac{2E_c}{T_c}}w_u\left(n+i\cdot\dfrac{N_c}{SF_f^u}\right)H_u\left(n+i\cdot\dfrac{N_c}{SF_f^u}\right) \\ \qquad\qquad \text{for MC-CDMA} \end{cases} \tag{26}$$

$$\xi_{MAI}(n) = \begin{cases} \dfrac{1}{SF_f^u}\displaystyle\sum_{t=nSF_f^u}^{(n+1)SF_f^u-1}\left\{c_u^{SF_f^u}(t)c_u^{scr}(t)\right\}^* \dfrac{1}{N_c}\sum_{k=0}^{N_c-1} w_u(k) \\ \qquad \times\left[\sqrt{\dfrac{2E_c}{T_c}}\displaystyle\sum_{\substack{u'=0,\\ \neq u}}^{U-1} S_{u'}(k)Z_{u'}(k)\right]\exp\left(j2\pi t\dfrac{k}{N_c}\right) \\ \qquad\qquad \text{for DS-CDMA} \\ \dfrac{1}{SF_f^u}\displaystyle\sum_{i=0}^{SF_f^u-1}\left\{c_u^{SF_f^u}(i)c_u^{scr}(n\cdot SF_f^u+i)\right\}^* w_u\left(n+i\cdot\dfrac{N_c}{SF_f^u}\right) \\ \qquad \times\left[\sqrt{\dfrac{2E_c}{T_c}}\displaystyle\sum_{\substack{u'=0\\ \neq u}}^{U-1} S_{u'}\left(n+i\cdot\dfrac{N_c}{SF_f^u}\right)Z_{u'}\left(n+i\cdot\dfrac{N_c}{SF_f^u}\right)\right] \\ \qquad\qquad \text{for MC-CDMA} \end{cases} \tag{27}$$

$$\xi_{noise}(n) = \begin{cases} \dfrac{1}{SF_f^u}\displaystyle\sum_{t=nSF_f^u}^{(n+1)SF_f^u-1}\left\{c_u^{SF_f^u}(t)c_u^{scr}(t)\right\}^* \\ \qquad \times\dfrac{1}{N_c}\displaystyle\sum_{k=0}^{N_c-1} w_u(k)\Pi_u(k)\exp\left(j2\pi t\dfrac{k}{N_c}\right) \\ \qquad\qquad \text{for DS-CDMA} \\ \dfrac{1}{SF_f^u}\displaystyle\sum_{i=0}^{SF_f^u-1}\left\{c_u^{SF_f^u}(i)c_u^{scr}\left(n\cdot SF_f^u+i\right)\right\}^* \\ \qquad \times w_u\left(n+i\cdot\dfrac{N_c}{SF_f^u}\right)\Pi_u\left(n+i\cdot\dfrac{N_c}{SF_f^u}\right) \\ \qquad\qquad \text{for MC-CDMA} \end{cases} \tag{28}$$

4.2 Variance

Since $\xi_{SI}(n)$ and $\xi_{MAI}(n)$ are approximated as complex Gaussian variables, the sum of $\xi_{SI}(n)$, $\xi_{MAI}(n)$ and $\xi_{noise}(n)$ can be treated as a new zero-mean Gaussian variable $\xi_{u,v}(n)$. Its variance $2\sigma_{u,v}^2(n)$ is given by

$$2\sigma_{u,v}^2(n) = 2\sigma_{SI}^2 + 2\sigma_{MAI}^2 + 2\sigma_{noise}^2, \tag{29}$$

where σ_{SI}^2, σ_{MAI}^2 and σ_{noise}^2 are the variances of $\xi_{SI}(n)$, $\xi_{MAI}(n)$, and $\xi_{noise}(n)$, respectively. Following [26], they can be derived as

$$2\sigma_{SI}^2 = \begin{cases} \dfrac{V}{SF_f^u}\dfrac{2E_c}{T_c}\left[\dfrac{1}{N_c}\displaystyle\sum_{k=0}^{N_c-1}|w_u(k)H_u(k)|^2 - \left|\dfrac{1}{N_c}\sum_{k=0}^{N_c-1} w_u(k)H_u(k)\right|^2\right] \\ \qquad\qquad \text{for DS-CDMA} \\ \dfrac{(V-1)}{SF_f^u}\dfrac{2E_c}{T_c} \\ \quad \times\left[\begin{array}{l} \dfrac{1}{SF_f^u}\displaystyle\sum_{i=0}^{SF_f^u-1}\left|w_u\left(n+i\cdot\dfrac{N_c}{SF_f^u}\right)H_u\left(n+i\cdot\dfrac{N_c}{SF_f^u}\right)\right|^2 \\ -\left|\dfrac{1}{SF_f^u}\displaystyle\sum_{i=0}^{SF_f^u-1} w_u\left(n+i\cdot\dfrac{N_c}{SF_f^u}\right)H_u\left(n+i\cdot\dfrac{N_c}{SF_f^u}\right)\right|^2 \end{array}\right] \\ \qquad\qquad \text{for MC-CDMA} \end{cases} \tag{30}$$

$$2\sigma_{MAI}^2 = \begin{cases} \dfrac{\sigma_Z^2}{SF_f^u}\dfrac{2E_c}{T_c}\left[\dfrac{1}{N_c}\displaystyle\sum_{k=0}^{N_c-1}|w_u(k)|^2\right] \\ \qquad\qquad \text{for DS-CDMA} \\ \dfrac{\sigma_Z^2}{SF_f^u}\dfrac{2E_c}{T_c}\left[\dfrac{1}{SF_f^u}\displaystyle\sum_{i=0}^{SF_f^u-1}\left|w_u\left(n+i\cdot\dfrac{N_c}{SF_f^u}\right)\right|^2\right] \\ \qquad\qquad \text{for MC-CDMA} \end{cases} \tag{31}$$

$$2\sigma_{noise}^2 = \begin{cases} \dfrac{1}{SF_t^uSF_f^u}\dfrac{2N_0}{T_c}\left[\dfrac{1}{N_c}\displaystyle\sum_{k=0}^{N_c-1}|w_u(k)|^2\right] \\ \qquad\qquad \text{for DS-CDMA} \\ \dfrac{1}{SF_t^uSF_f^u}\dfrac{2N_0}{T_c}\left[\dfrac{1}{SF_f^u}\displaystyle\sum_{i=0}^{SF_f^u-1}\left|w_u\left(n+i\cdot\dfrac{N_c}{SF_f^u}\right)\right|^2\right] \\ \qquad\qquad \text{for MC-CDMA} \end{cases} \tag{32}$$

In Eq. (31), $2\sigma_Z^2$ is the variance of $Z_{u'}(k)$ defined in Eq. (23). Since $h_{u,l}(\lfloor t/T \rfloor)$ and $h_{u',l}(\lfloor t/T \rfloor)$ are zero-mean compelx Gaussian processes, $H_u(k)$ and $Z_{u'}(k)$ are also zero-mean complex Gaussian variables. Therefore, the second term in Eq. (22) can be approximated as a zero-mean complex Gaussian variable with variance $(2E_c/T_c)\sigma_Z^2$, where σ_Z^2 is defined as

$$\sigma_Z^2 = E\left[\left|\sum_{\substack{u'=0\\ \neq u}}^{U-1} S_{u'}(k)Z_{u'}(k)\right|^2\right]. \tag{33}$$

$S_{u'}(k)$ is the frequency component of the u'th user's signal $s_{u'}(t)$ and is a zero-mean variable with the variance of $E[|S_{u'}(k)|^2] = 1$ (this can be derived from Eq. (23) since a binary scramble sequence is assumed). Since $S_{u'}(k)$ is independent of $Z_{u'}(k)$, we have

$$\sigma_Z^2 = \sum_{\substack{u'=0\\ \neq u}}^{U-1} E[|Z_{u'}(k)|^2]. \tag{34}$$

We assume the Jake's model [27] and each path consists of many unresolvable paths with the same time delay arriving from all directions uniformly. From Eq. (23), Eq. (34) becomes

$$\begin{aligned}\sigma_Z^2 &= \sum_{\substack{u'=0\\ \neq u}}^{U-1} \frac{1}{(SF_t^u)^2} \sum_{i'=0}^{SF_t^u-1}\sum_{i=0}^{SF_t^u-1} \left\{ J_0\left(2\pi\left|i-i'\right| f_D^{(u')}T\right)\right.\\ &\quad \left.\times\left[c_{u'}^{SF_t^{u'}}(i)c_u^{SF_t^u}(i')\left\{c_{u'}^{SF_t^{u'}}(i')c_u^{SF_t^u}(i)\right\}^*\right]\right\}\\ &\approx \frac{1}{SF_t^u}\sum_{\substack{u'=0\\ \neq u}}^{U-1}\sum_{\Delta i=1-SF_t^u}^{SF_t^u-1} J_0(2\pi|\Delta i| f_D^{(u')}T),\end{aligned} \tag{35}$$

where $f_D^{(u')}$ is the u'th user's maximum Doppler frequency and $J_0(\cdot)$ is the zero-th order Bessel function of the first kind. It is understood that σ_Z^2 is the sum of the weighted cross-correlations of the OVSF spreading codes $\{c_u^{SF_t^u}(t);\ u = 0 \sim U-1\}$. If $f_D^{(u')} = 0$, σ_Z^2 beomes zero due to the orthogonality property of the OVSF spreading codes. Therefore, the MAI between different groups can be eliminated completely.

In the case of single connection ($V = 1$), it can be understood from Eq. (30) that there is no SI for MC-CDMA but SI still exists for DS-CDMA. In the case of DS-CDMA, even with MMSE-FDE, variations in the equivalent channel gain, defined as $w_u(k)H_u(k)$, still remain. This residual variation produces the SI, which is not negligible when V is large. However, note that the BER performance difference between DS- and MC-CDMA diminishes as SF_f^u approaches N_c.

4.3 Conditional BER

The conditional signal-to-interference plus noise ratio (SINR) $\gamma(E_c/N_0, \{H_u(k)\})$ for the given set of $\{H_u(k);\ k = 0 \sim N_c-1\}$ is defined as

$$\gamma\left(\frac{E_c}{N_0}, \{H_u(k)\}\right) = \frac{\left|\mu_{u,v}(n)\right|^2}{\sigma_{u,v}^2(n)}. \tag{36}$$

Assuming QPSK data-modulation, the conditional BER is then given by [28]

$$P_b\left(\gamma\left(\frac{E_c}{N_0}, \{H_u(k)\}\right)\right) = \frac{1}{2}erfc\sqrt{\frac{1}{4}\gamma\left(\frac{E_c}{N_0}, \{H_u(k)\}\right)}. \tag{37}$$

The theoretical average BER of uncoded CDMA can be numerically evaluated by averaging Eq. (4) over $\{H_u(k);\ k = 0 \sim N_c-1\}$ as

$$P_b\left(\frac{E_c}{N_0}\right) = E\left[P_b\left(\gamma\left(\frac{E_c}{N_0}, \{H_u(k)\}\right)\right)\right]. \tag{38}$$

5. Simulation Results

The numerical and computer simulation conditions are shown in Table 1. An $L = 16$-path frequency-selective block Rayleigh fading channel having the uniform power delay profile is assumed. The transmit timing offsets $\{\tau_u;\ u = 0 \sim U-1\}$ are uniformly distributed over $[-\Delta/2, \Delta/2]$ with $\Delta < N_g - L$ so that the maximum time delay difference is less than the GI. A rate-1/3 turbo encoder consists of two (13, 15) recursive systematic convolutional (RSC) encoders [23] connected in parallel with an S-random ($S = \sqrt{I}$) interleaver [29] between them. The input to the second RSC encoder is the interleaved version of the information sequence input to the first RSC encoder. The following puncturing matrix P is used to get a rate-1/2 turbo code:

$$P = \begin{bmatrix} 1 & 1\\ 1 & 0\\ 0 & 1\end{bmatrix}, \tag{39}$$

where the first row corresponds to the systematic (or information) bit sequence, and the second and third rows correspond to the two parity bit sequences. The turbo decoder is an iterative decoder. The log-MAP decoding with eight iterations is carried out at the turbo decoder.

The numerical evaluation of the theoretical average BER is done by Monte-Carlo numerical computation method as follows. The set of path gains $\{h_{u,l}(\lfloor t/T\rfloor);\ l = 0 \sim L-1\}$ for different users are generated to obtain $\{H_u(k);\ k = 0 \sim N_c-1\}$ using Eq. (23) and then $\{w_u(k);\ k = 0 \sim N_c-1\}$ using Eq. (9). The conditional BER is

Table 1 Numerical and simulation conditions.

Trans-mitter	Turbo encoder	Data bit length I=1018
		Coding rate R=1/2
		(13,15) RSC encoder
		S-random interleaver
	Modulation	QPSK
	2D OVSF spreading	SF_f^u=1~256, SF_t^u=1~16
	Block length	N_c=256
	GI	N_g=32
Recei-ver	Channel esti.	Ideal
	Turbo decoder	Log-MAP
		8 iterations

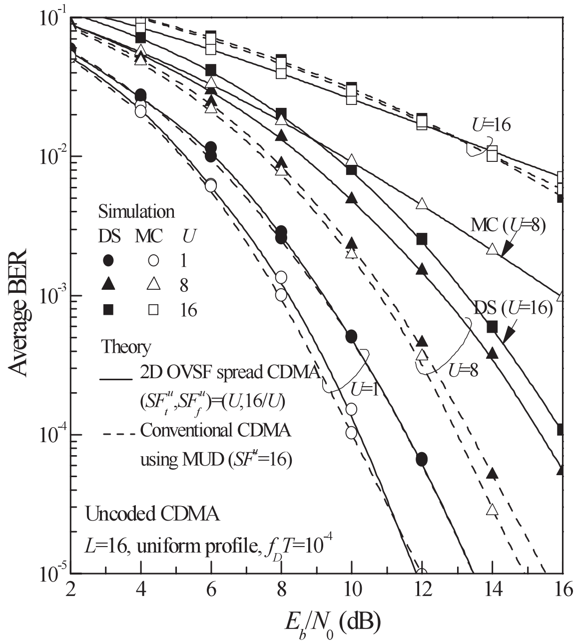

Fig. 7 Uncoded BER comparison between 2D OVSF spread CDMA and conventional CDMA using MUD.

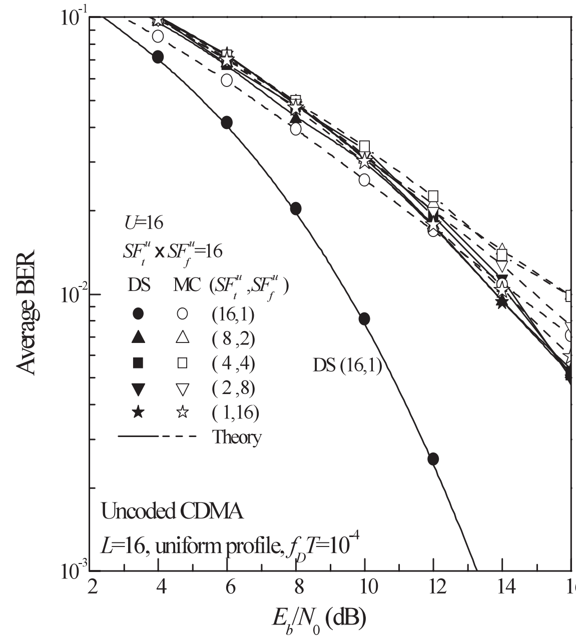

Fig. 8 Uncoded BER performance of 2D OVSF spread CDMA for various pairs of (SF_t, SF_f) with $SF_t^u \times SF_f^u = 16$.

computed using Eqs. (41) and (42). This is repeated a sufficient number of times to obtain the theoretical average BER according to Eq. (38).

5.1 Uncoded Case

We first consider the $V = 1$ case. Fig. 7 plots the uncoded BER performance of both DS- and MC-CDMA as a function of the average received bit energy-to-the AWGN power spectrum density ratio E_b/N_0, defined by $E_b/N_0 = 0.5(E_c/N_0)(SF_t^u SF_f^u) \times (1 + N_g/N_c)$ with $f_D T = 10^{-4}$ for all users. For comparison, the BER performance of conventional CDMA using MMSE-MUD [12] is also plotted for $U = 1$, 8 and 16 ($R_{total} = 1/16$, 1/2 and 1). We assume the spreading factor of $SF^u = SF_t^u \times SF_f^u = 16$ for 2D OVSF spread CDMA, where $(SF_t^u, SF_f^u) = (U, 16/U)$, and the same spreading factor of $SF^u = 16$ for conventional CDMA using MUD. The good agreement between the theoretical and simulation results confirms our BER analysis. Our proposed 2D OVSF spread CDMA is an MAI-free system due to $\sigma_Z^2 = 0$ (see Eqs. (31) and (36)) since all the users with $SF_t^u = U$ are orthogonal and the channel is almost constant when the fading is very slow ($f_D T = 10^{-4}$). The MUD problem is converted into a set of equivalent single-user detection problems and only single-user MMSE-FDE is applied here. On the other hand, for conventional CDMA, MUD is necessary to combat the MAI. When the system is lightly loaded (i.e., $U = 8$), conventional DS-CDMA using MUD exhibits better performance since the MAI is less severe. However, when the system is heavily loaded (i.e., $U \approx SF^u$), large MAI results in severe BER degradation for conventional DS-CDMA with MUD. When $U = 16$, our proposed 2D OVSF spread DS-CDMA outperforms conventional DS-CDMA with MUD.

In 2D OVSF spread DS-CDMA, the data symbol is always spread over all subcarriers, yielding large frequency diversity gain irrespective of SF_f^u. However, DS-CDMA suffers from SI, the variance of which is in inverse proportion of SF_f^u. On the other hand, in the case of MC-CDMA, the data symbol is spread over smaller number (equal to SF_f^u) of subcarriers than in DS-CDMA, the frequency diversity gain is in linear proportion of SF_f^u. But MC-CDMA can achieve a large frequency-domain interleaving gain and there is no SI present when $V = 1$. When $U = 1$ ($SF_f^u = 16$), 2D OVSF spread MC-CDMA performs slightly better than DS-CDMA. As U increases, SF_f^u decreases, resulting in less frequency-diversity gain in MC-CDMA and increasing SI in DS-CDMA. It can be seen that the BER performances of both 2D OVSF spread DS- and MC-CDMA degrade as U increases. When $U = 16$ ($SF_f^u = 1$), 2D OVSF spread DS-CDMA provides much better BER performance than MC-CDMA. This is because that there is neither frequency-diversity gain nor interleaving gain in 2D OVSF spread MC-CDMA without coding; while, although there is SI in 2D OVSF spread DS-CDMA, larger frequency-diversity gain can be obtained in DS- than that in MC-CDMA.

Figure 8 plots the uncoded BER performance of both DS- and MC-CDMA assuming that all users have the same spreading factor pair, i.e., $(SF_t^u, SF_f^u) = (SF_t, SF_f)$. We assume a full-loaded case (i.e., $U = SF_t \times SF_f = 16$) with the same data rate for all users. As explained in Sect. 3, if $SF_t < U$, users are partitioned into SF_t groups. Users in each group are interference-free from other groups; but the MAI is present in each group and MUD is applied per group. As the number of users per group, U/SF_t, increases,

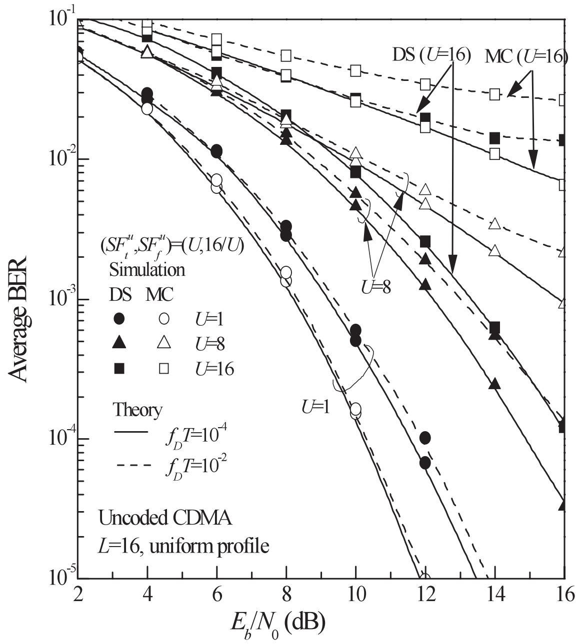

Fig. 9 Impact of f_DT on uncoded 2D OVSF spread CDMA.

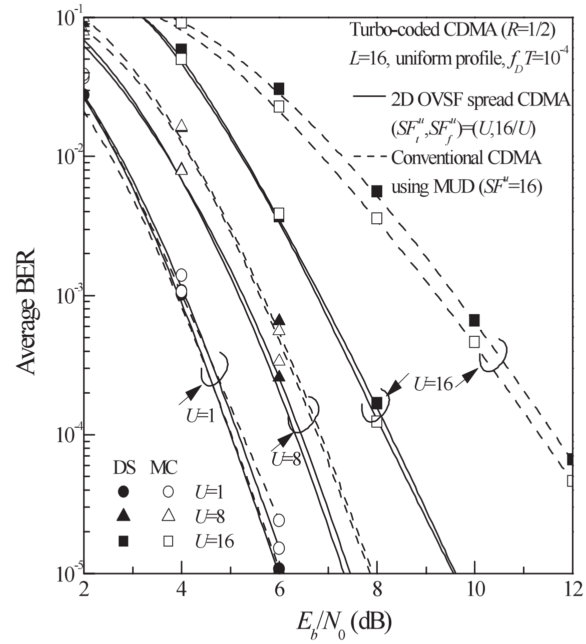

Fig. 10 Coded performance comparison between 2D OVSF spread CDMA and conventional CDMA using MUD.

the residual MAI per group increases, resulting in the degradation of the BER performance. It is necessary to apply MMSE-MUD per group to combat with this residual MAI and its implementation complexity increases exponentially with U/SF_t. When $(SF_t, SF_f) = (16, 1)$, the MAI can be eliminated completely and single-user MMSE-FDE is applied instead of complicated MMSE-MUD. It is seen form Fig. 8 that DS-CDMA with $(SF_t, SF_f) = (16, 1)$ performs better than that of $(SF_t, SF_f) \neq (16, 1)$. Therefore, the use of $(SF_t^u, SF_f^u) = (U, SF^u/U)$ can achieve the best BER performance with the lowest receiver complexity. However, MC-CDMA with $(SF_t, SF_f) = (16, 1)$ does not give a good BER performance similar to DS-CDMA. This is because MC-CDMA with $(SF_t, SF_f) = (16, 1)$ cannot obtain the frequency-diversity gain if error-control coding is not used.

How the fading Doppler frequency influences the BER performance is shown for $SF_t^u \times SF_f^u = 16$ and $(SF_t^u, SF_f^u) = (U, 16/U)$ in Fig. 9. Both the theoretical and simulated BER performances are plotted for the uncoded CDMA with single connection $V = 1$ and multiple users. We assume the same fading Doppler spread $f_DT = 10^{-4}$ and 10^{-2} for all users (corresponding to the mobile terminal speed of about 7 km/h and 700 km/h, respectively, for the carrier frequency 5 GHz and the chip data rate 100 Mcps). It can be seen that the theoretical results agree well with those of computer simulation. For small number of users (i.e., $U = 1$ or 8), there is only a slight performance difference between $f_DT = 10^{-4}$ and $f_DT = 10^{-2}$. However, when $f_DT = 10^{-2}$, since the orthogonality among different users cannot be maintained due to the time-selective fading, the performances of both uncoded DS- and MC-CDMA degrade for the heavy-loaded case (i.e., $U = 16$).

5.2 Turbo-Coded Case

Turbo-coded BER performance comparison between conventinal CDMA using MUD with $SF^u = 16$ and 2D OVSF spread CDMA with $(SF_t^u, SF_f^u) = (U, 16/U)$ for $SF_t^u \times SF_f^u = 16$ is shown in Fig. 10. In contrast to the uncoded case shown in Fig. 7, due to the coding gain together with frequency-diversity and interleaving gain, 2D OVSF spread/chip-interleaved MC-CDMA can achieve almost the same BER performance as the DS-CDMA even for small SF_f^u (i.e., $U = 8$ and 16). Also 2D OVSF spread CDMA provides better performance than conventional CDMA with MUD. Moreover, although the computational complexity of MUD grows exponentially with the number of users U, the receiver complexity of 2D OVSF spread CDMA is linear due to the use of single-user FDE.

Figure 11 plots the turbo-coded BER performance of full-loaded CDMA ($U = 16$) with different spreading factor pair $(SF_t^u, SF_f^u) = (SF_t, SF_f)$ for all users. Similar to the case of Fig. 8, U users are partitioned into SF_t groups if $SF_t < U$. Each group is interference-free from other groups. However, since $SF_t < U$, some groups have more-than-one users; the MAI is present in those groups and MUD is necessary to combat the residual MAI. Compared with the uncoded case in Fig. 8, turbo-coded MC-CDMA can achieve a similar performance to DS-CDMA for different (SF_t, SF_f) pair and 2D OVSF spread CDMA with turbo coding provides different BER performance for various (SF_t, SF_f). 2D OVSF spread CDMA with $(SF_t, SF_f) = (16, 1)$ performs the best by using only single-user MMSE-FDE. As SF_t decreases, the BER performance degrades due to the increasing residual MAI from U/SF_t users. When $(SF_t, SF_f) = (1, 16)$, 2D OVSF

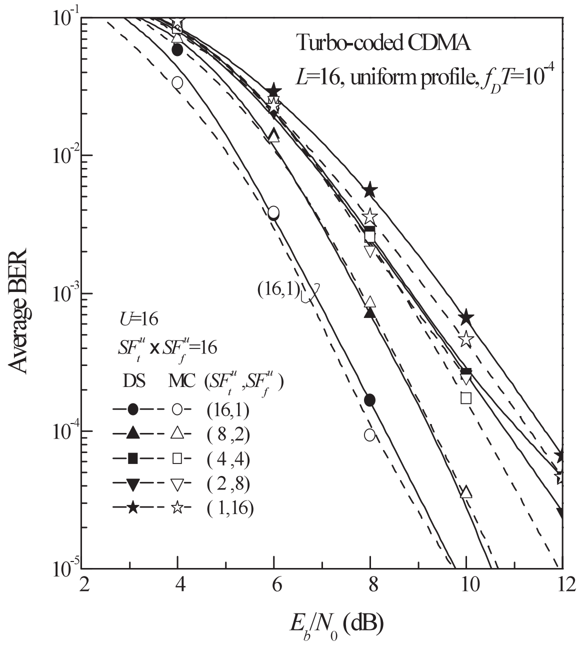

Fig. 11 Turbo-coded BER performance of 2D OVSF spread CDMA for various pairs of (SF_t, SF_f).

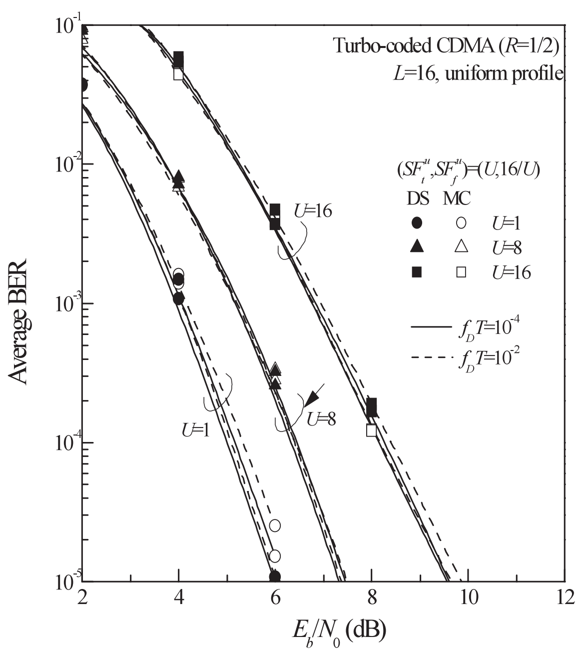

Fig. 12 Impact of f_DT on turbo-coded 2D OVSF spread CDMA.

spread CDMA reduces to conventional CDMA, which uses the most complicated MMSE-MUD but performs worse than 2D OVSF spread CDMA with $(SF_t, SF_f) \neq (16, 1)$.

The impact of the fading Doppler frequency on the BER performance was shown in Fig. 9 for the uncoded case. Assuming the same conditions, we show in Fig. 12 the turbo-coded BER performance for $f_DT = 10^{-4}$ and $f_DT = 10^{-2}$. It can be seen that our proposed 2D OVSF CDMA with turbo coding is very robust against large Doppler

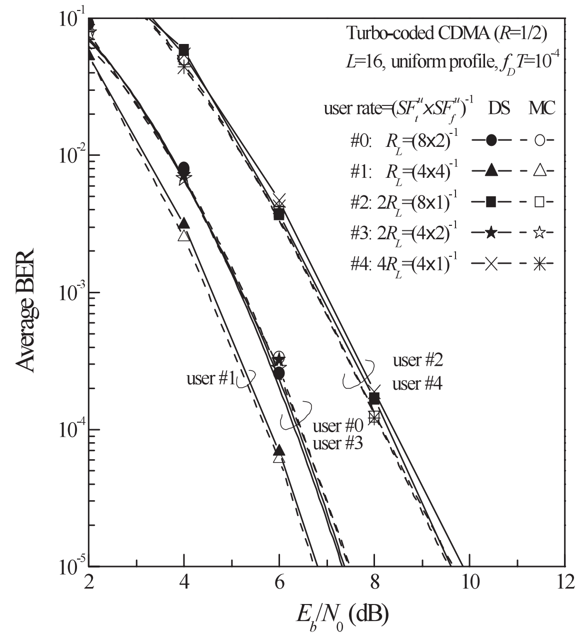

Fig. 13 Turbo-coded BER performance of multi-rate/single-connection 2D OVSF spread CDMA.

spread. The chip-interleaving performs like a channel interleaving for turbo-coded CDMA [30]. Chip interleaving scrambles the chips and transforms the transmission channel into a highly time-selective or highly memoryless channel. There is a tradeoff between the residual MAI and the interleaving gain for the turbo decoding. Therefore, our 2D OVSF spread/chip-interleaved CDMA with turbo coding is insensitive of the Doppler spread compared with uncoded case.

5.3 Mutli-Rate/Multi-Connection Case

Figure 13 plots the turbo-coded BER performance of the mutli-rate case with $U = 5$, $R_{total} = 0.625$ and the lowest data rate $R_L = 1/16$. As described in Sect. 3.1.3, the data rates of users $u = 0 \sim 4$ are R_L, R_L, $2R_L$, $2R_L$ and $4R_L$, respectively. User $u = 2$ with $(SF_t^2, SF_f^2) = (8, 1)$ and user $u = 4$ with $(SF_t^4, SF_f^4) = (4, 1)$ have different data rates but show the same BER performance, which is worse than that of users $u = 0$ and 3. User $u = 0$ with $(SF_t^0, SF_f^0) = (8, 2)$ and user $u = 3$ with $(SF_t^3, SF_f^3) = (4, 2)$ with different data rates also performs the same, but their BER performances are still worse then user $u = 1$ with $(SF_t^1, SF_f^1) = (4, 4)$. It can be seen that if SF_f^u is the same, the BER performance is the same irrespective of data rate. However, as SF_f^u decreases, the BER performances of both 2D OVSF spread DS- and MC-CDMA degrade. The reason for this has been discussed in Sect. 5.1.

The BER performance of turbo-coded CDMA with multi-rate/multi-connection is shown for $SF_f^u = U = 16$ in Fig. 14. We assume different equivalent spreading factors, $SF_{f,eq}^u = 1$, 2 and 16 ($R_{total} = 1$, 1/2, and 1/6). In

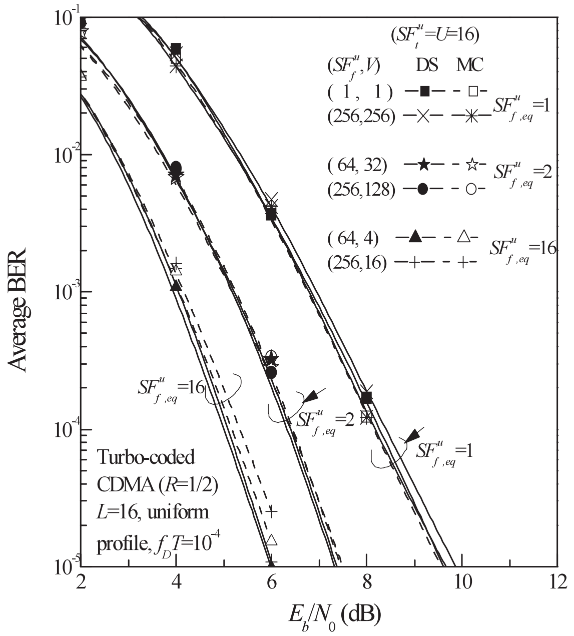

Fig. 14 Turbo-coded BER performance of multi-rate/multi-connection 2D OVSF spread CDMA.

the case of $SF^u_{f,eq} = 1$, we consider $(SF^u_f, V) = (1, 1)$ and $(256, 256)$. Both $(SF^u_f, V) = (64, 32)$ and $(256, 128)$ correspond to the case of $SF^u_{f,eq} = 2$; while, $(SF^u_f, V) = (64, 4)$ and $(256, 16)$ correspond to the case of $SF^u_{f,eq} = 16$. MC-CDMA with turbo coding can achieve almost the same BER performance as DS-CDMA for different (SF^u_f, V). The multi-connection CDMA with $(SF^u_f, V) = (256, 256)$ shows the identical BER performance to that of single-connection CDMA with $(SF^u_f, V) = (1, 1)$ since they have the same $SF^u_{f,eq} (= 1)$. According to the BER analysis in Sect. 4, we can see by substituting Eqs. (25), (29)–(32) into Eq. (36) that if $SF^u_{f,eq}$ is the same, the conditional SINR for the multi-connection CDMA are the same as that of the single-connection CDMA. Multi-connection CDMA with the same $SF^u_{f,eq}$ presents the same BER performance; however, 2D OVSF spread CDMA with different $SF^u_{f,eq}$ has different R_{total} and exhibits different BER performance.

6. Conclusions

In this paper, we proposed a 2-dimensional (2D) OVSF spread/chip-interleaved CDMA in a frequency-selective fading channel for multi-rate uplink transmission. Code assignment for 2D OVSF spreading was presented. Relying on the joint use of 2D OVSF spreading and chip-interleaving, a multiuser detection (MUD) problem is converted into a set of equivalent single-user equalization problems. The suppression of multi-access interference (MAI) not only increases the uplink capacity without applying the sophisticated MUD technique, but also allows flexible multi-rate transmission using our proposed 2D OVSF spreading code assignment. We also presented the theoretical analysis for the uncoded BER performance based on the Gaussian approximation of the MAI. The theoretical uncoded BER performance in a time- and frequency-selective Rayleigh fading channel was evaluated by Monte-Carlo numerical computation and confirmed by computer simulation. It was also shown by simulation results that when turbo coding is applied, our proposed 2D OVSF spread/chip-interleaved DS- and MC-CDMA can achieve similar BER performance and are very robust against large Doppler spread.

References

[1] F. Adachi, "Wireless past and future-Evolving mobile communications systems," IEICE Trans. Fundamentals, vol.E84-A, no.1, pp.55–60, Jan. 2001.
[2] F. Adachi, D. Garg, S. Takaoka, and K. Takeda, "Broadband CDMA techniques," IEEE Wireless Commun., vol.12, no.2, pp.8–18, April 2005.
[3] A.J. Viterbi, CDMA: Principles of spread spectrum communications, Addison Wesley, 1995.
[4] T. Ottosson and A. Svensson, "On schemes for multirate support in DS/CDMA," J. Wireless Personal Commun., vol.6, no.3, pp.265–287, March 1998.
[5] F. Adachi, "Reverse link capacity of orthogonal multi-code DS-CDMA with multiple connections," IEICE Trans. Commun., vol.E85-B, no.11, pp.2520–2526, Nov. 2002.
[6] F. Adachi, T. Sao, and T. Itagaki, "Performance of multicode DS-CDMA using frequency domain equalization in a frequency selective fading channel," Electron. Lett., vol.39, no.2, pp.239–241, Jan. 2003.
[7] S. Hara and R. Prasad, "Overview of muticarrier CDMA," IEEE Commun. Mag., vol.35, no.12, pp.126–144, Dec. 1997.
[8] L.-L. Yang and L. Hanzo, "Multicarrier DS-CDMA: A multiple access scheme for ubiquitous broadband wireless communications," IEEE Commun. Mag., vol.41, no.10, pp.116–124, Oct. 2003.
[9] S. Hara and R. Prasad, "Design and performance of multicarrier CDMA system in frequency-selective Rayleigh fading channels," IEEE Trans. Veh. Technol., vol.48, no.5, pp.1584–1595, Sept. 1999.
[10] M. Helard, R. Le Gouable, J.-F. Helard, and J.-Y. Baudais, "Multicarrier CDMA techniques for future wideband wireless networks," Ann. Telecommun., vol.56, pp.260–274, 2001.
[11] Z. Wang and G.B. Giannakis, "Block precoding for MUI/ISI-resilient generalized multicarrier CDMA with multirate capabilities," IEEE Trans. Commun., vol.49, no.11, pp.2016–2027, Nov. 2001.
[12] S. Tsumura, S. Hara, and Y. Hara, "Performance comparison of MC-CDMA and cyclically prefixed DS-CDMA in an uplink channel," Proc. IEEE VTC'04 Fall, pp.414–418, Los Angeles, USA, Sept. 2004.
[13] X.D. Wang and H.V. Poor, "Iterative (turbo) soft interference cancellation and decoding for coded CDMA," IEEE Trans. Commun., vol. 47, no.7, pp.1046–1061, July 1999.
[14] S. Parkvall, E. Strom, and B. Ottersten, "The impact of timing errors on the performance of linear DS-CDMA receivers," IEEE J. Sel. Areas Commun., vol.14, no.8, pp.1660–1668, Oct. 1996.
[15] H. Atarashi, N. Maeda, Y. Kishiyama, and M. Sawahashi, "Broadband wireless access based on VSF-OFCDM and VSCRF-CDMA and its experiments," European Trans. Telecommun., vol.15, pp.159–172, Jan. 2004.
[16] S. Zhou, G.B. Giannakis, and C.L. Martret, "Chip-interleaved block-spread code division multiple access," IEEE Trans. Commun., vol.50, no.2, pp.235–248, Feb. 2002.
[17] X. Peng, F. Chin, T.T. Tjhung, and A.S. Madhukumar, "A simplified transceiver structure for cyclic extended CDMA system with fre-

quency domain equalization," Proc. IEEE VTC'05 Spring, pp.1565–1569, Sweden, May 2005.
[18] F. Adachi, M. Sawahashi, and K. Okawa, "Tree-structured generation of orthogonal spreading code with different lengths for foward link of DS-CDMA mobile radio," Electron. Lett., vol.33, no.1, pp.27–28, Jan. 1997.
[19] K. Okawa and F. Adachi, "Orthogonal forward link using orthogonal multi-spreading factor codes for coherent DS-CDMA mobile radio," IEICE Trans. Commun., vol.E81-B, no.4, pp.777–784, April 1998.
[20] L. Liu and F. Adachi, "Chip-interleaved DS-CDMA with 2-dimansional OVSF spreading codes," IEICE Technical Report, RCS2004-372, pp.33–38, March 2005.
[21] L. Liu and F. Adachi, "2-dimensional OVSF spreading for chip-interleaved DS-CDMA uplink transmission," Proc. WPMC05, pp.576–580, Alborg, Denmark, Sept. 2005.
[22] A. Stefanov and T. Duman, "Turbo coded modulation for wireless communications with antenna diversity," Proc. IEEE VTC'99 Fall, pp.1565–1569, Netherlands, Sept. 1999.
[23] J.P. Woodard and L. Hanzo, "Comparative study of turbo decoding techniques: An overview," IEEE Trans. Veh. Technol., vol.49, no.6, pp.2208–2233, Nov. 2000.
[24] T.S. Rappaport, Wireless Communications, Prentice Hall, 1996.
[25] D. Garg and F. Adachi, "Throughput comparison of turbo-coded HARQ in OFDM, MC-CDMA and DS-CDMA with frequency-domain equalization," IEICE Trans. Commun., vol.E88-B, no.2, pp.664–677, Feb. 2005.
[26] F. Adachi and K. Takeda, "Bit error rate analysis of DS-CDMA with joint frequency-domain equalization and antenna diversity combining," IEICE Trans. Commun., vol.E87-B, no.10, pp.2991–3002, Oct. 2004.
[27] W.C. Jakes, Microwave Mobile Communications, Wiley, New York, 1974.
[28] J.G. Proakis, Digital Communications, 3rd ed., McGraw-Hill, New York, 1995.
[29] O.F. Acikel and W.E. Ryan, "Punctured turbo codes for BPSK/QPSK channels," IEEE Trans. Commun., vol.47, no.9, pp.1315–1323, Sept. 1999.
[30] D. Garg and F. Adachi, "Chip interleaved turbo codes for DS-CDMA mobile radio in a fading channel," Electron. Lett., vol.38, no.13, pp.642–644, June 2002.

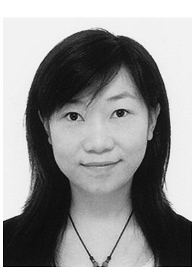

Le Liu received B.S. and M.S. degrees in electrical engineering from Beijing University of Posts and Telecommunications (BUPT), Beijing, China, in 2000 and 2003, respectively. From April 2003 to September 2004, she took part in the collaboration between the National Institute of Information and Communications Technology (NICT), Japan, and BUPT on the 4G Wireless Telecommunications Project. Currently, she is a Ph.D. candidate at the Dept. of Electrical and Communication Engineering, Graduate School of Engineering, Tohoku University with a scholarship from the Japanese government. Her research interests include digital signal transmission techniques for direct sequence CDMA and multicarrier CDMA.

Fumiyuki Adachi received the B.S. and Dr. Eng. degrees in electrical engineering from Tohoku University, Sendai, Japan, in 1973 and 1984, respectively. In April 1973, he joined the Electrical Communications Laboratories of Nippon Telegraph & Telephone Corporation (now NTT) and conducted various types of research related to digital cellular mobile communications. From July 1992 to December 1999, he was with NTT Mobile Communications Network, Inc. (now NTT DoCoMo, Inc.), where he led a research group on wideband/broadband CDMA wireless access for IMT-2000 and beyond. Since January 2000, he has been with Tohoku University, Sendai, Japan, where he is a Professor of Electrical and Communication Engineering at the Graduate School of Engineering. His research interests are in CDMA wireless access techniques, equalization, transmit/receive antenna diversity, MIMO, adaptive transmission, and channel coding, with particular application to broadband wireless communications systems. From October 1984 to September 1985, he was a United Kingdom SERC Visiting Research Fellow in the Department of Electrical Engineering and Electronics at Liverpool University. Dr. Adachi served as a Guest Editor of IEEE JSAC for special issue on Broadband Wireless Techniques, October 1999 and for special issue on Wideband CDMA I, August 2000, and Wideband CDMA II, Jan. 2001. He is an IEEE Fellow and was a co-recipient of the IEEE Vehicular Technology Transactions Best Paper of the Year Award 1980 and again 1990 and also a recipient of Avant Garde award 2000. He was a recipient of IEICE Achievement Award 2002 and a co-recipient of the IEICE Transactions Best Paper of the Year Award 1996 and again 1998. He was a recipient of Thomson Scientific Research Front Award 2004.